resources

MDPI

Article

Development of Alloyed Pipe Steel Composition for Oil and Gas Production in the Arctic Region

Pavel Poletskov [1], Marina Gushchina [1], Marina Polyakova [1,*], Daniil Alekseev [1], Olga Nikitenko [1], Dmitrii Chukin [1] and Yuri Vasil'ev [2]

[1] Department of Material processing, Nosov Magnitogorsk State Technical University, Magnitogorsk 455000, Russia; p.poletskov@magtu.ru (P.P.); gushchina.ms@mail.ru (M.G.); d.u.alekseev@mail.ru (D.A.); o.nikitenko@magtu.ru (O.N.); chukindmitry@gmail.com (D.C.)

[2] Peter the Great St. Petersburg Polytechnic University, St. Petersburg 195251, Russia; president@spbstu.ru

* Correspondence: m.polyakova@magtu.ru; Tel.: +7-3519-298481

Received: 5 March 2019; Accepted: 3 April 2019; Published: 8 April 2019

Abstract: Gas and oil pipelines for the Arctic region must sustain low temperatures and high internal pressures of a corrosive active medium. Generation of new steel compositions for oil and gas pipelines is an urgent issue in order to ensure their high reliability. Low-carbon steels with a ferritic–pearlitic structure are normally used in pipe production, but they are unable to cope with increased market demands. The main objective of this study is to investigate the influence of the cooling rate on the structure and morphological characteristics of bainite, which determines the exploitation properties of the pipe steels. Dilatometric tests were carried out using a Gleeble 3500 complex. Optical microscope and scanning electron microscope analysis, with the computer image analysis system Thixomet PRO, were used to study the microstructure of steel. Hardness was measured in accordance with ASTM E-384. Morphological characteristics of bainite components that were formed at various cooling rates from 0.05 to 100 °C/s were defined. The novel result of this study is the continuous cooling transformation diagram of undercooled austenite of the steel containing 0.062% C; 1.80% Mn; 0.120% Mo; 0.032% Cr, 0.90% Ni and other elements (Al, Cu, V, Nb, Ti).

Keywords: gas and oil pipeline; low-carbon steel; microstructure; bainite; dilatometric test; undercooled austenite; continuous cooling transformation diagram

1. Introduction

Development of Arctic resources is a geopolitical issue influencing the development of the world economy and power generation in the near future. The territory of the Russian Federation includes a vast sea shelf, which makes up almost 22% of the total area of the world's ocean shelf, and 70% of this Russian sea shelf can be used to produce oil and gas. According to geological data, this territory contains about 56 billion tons of proven oil and gas resources and is forecasted to contain an extra 100–140 billion tons of oil and gas resources (in oil equivalents) [1,2]. For the Russian Federation, oil and gas production on the shelf of the northern seas and Sakhalin Island is an important strategic objective and, to a great extent, the economic situation in the country and its defense potential depends on whether this objective will be achieved. It should be noted that foreign companies lack experience in oil and gas production on ice. The solution to the problem of developing a sea ice-resistant platform for operation on the shelf of the arctic seas and Sakhalin Island has no parallels in the world practice [3,4].

Furthermore, the Northern Sea Route, the shortest passage for water traffic from Europe to Asia, which is twice as short as the route through the Suez Canal, follows the arctic coast of Russia. In accordance with the forecast data of the development strategy of the Arctic zone of the Russian

Federation and national security protection for the period through to 2020, and with the Fundamentals of the State Policy of the Russian Federation in the Arctic for the period up to 2020 and Beyond [5–7], the freight traffic along the Northern Sea Route will increase from 7.5 million tons to 60 million tons (Figure 1). The share of this region in the GDP of Russia is about 12%, while its share in the export of the country is about 25%. Meanwhile, warming in the Arctic region makes it possible to use the Northern Sea Route for international oil, compressed natural gas, and iron ore trade, which is why the demand for the services of the Russian icebreaker is growing steadily.

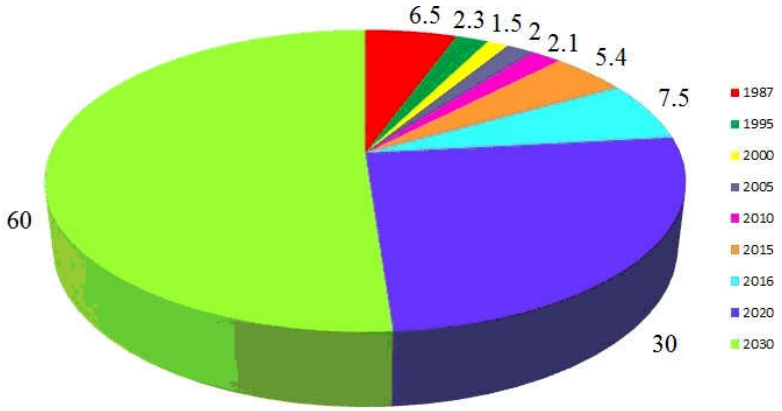

Figure 1. Dynamics of freight traffic volume along the Northern Sea Route (million tons).

A number of contracts have been signed with the world leading pipe-making companies to supply single-joint welded pipes for the construction of the subsea transfer pipeline Nord Stream 2 [8], which is intended to extend the gas transmission system within the framework of the gas pipeline construction (Figure 2).

Figure 2. Nord Stream 2: Nord Stream; Nord Stream 2 (planned)

The estimated demand of large diameter pipes is about 2.2 million tons. The gas pipeline Nord Stream 2 will go along the sea floor of the Baltic Sea from the Russian coast to the German coast near Greifswald. The throughput capacity of the two strings will be 55 billion cubic meters per annum (BCMPA). In order to be able to implement the project and to construct the section of the pipeline on the shore between the ground-surface and the subsea sections of the pipeline, it is necessary to produce low temperature pipes with an inside pipe diameter of 1153 mm and pipe wall thickness of 28.5 to 41.0 mm, with a shear area fraction at −38 °C no less than 90%, and the absorbed energy for the Charpy impact bending test at −48 °C no less than 170 J transversely and 250 J longitudinally.

To provide highly reliable gas and oil pipelines in adverse climatic conditions, the flat products intended for welded pipe production must have a high level of low temperature resilience, and higher resistance to brittle and ductile fractures at low temperatures at static, cyclic and dynamic loads. As a result, it is vitally important to develop the technology of skelp steel production and make it available, as it will be used to manufacture pipes for field infrastructure development projects in the Arctic. The need of making use of such steels became obvious, in the first place, due to natural resource development in the polar regions and on the Arctic shelf of the country [9–12], which is schematically presented in Figure 3.

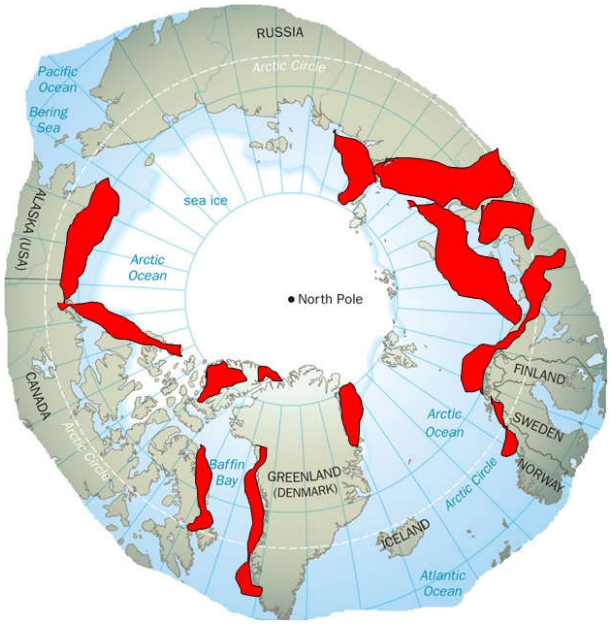

Figure 3. Deposit map in the Arctic.

The main feature of the current oil and gas complex is that its main production facilities are located in hard-to-reach areas of the Far North, which are remote from the industrial centers of the country. The new oil and gas deposits and the deposits under development are located at higher and higher latitudes and are characterized by more complex mining and geological structure. The opportunities of natural gas production are associated with a switch to hard-to-recover reserves and to the deposits located under complex geological conditions, which will result in an increase in demand for high-tech pipes, for both oil and gas production.

At the same time, growth in gas production is expected (by 1.1% in 2017, by 2.0% in 2018), meaning that Gazprom will start developing new deposits and the independent gas suppliers will increase gas production under the conditions of their equal-opportunity access to the Unified Gas Supply System [13–15]. It is expected that from 2016 to 2018 more than 813 billion rubles will be invested into production of natural gas and natural gas liquid [15].

Low-carbon alloyed steels with ferritic-pearlitic structure are widely used in pipe production. Experience has shown that when such structure is formed in low-carbon pipe steel, it is impossible to obtain strength properties higher than the K60 (X70) strength class combined with the required toughness, resistance to cold and weldability at the same time. To achieve this, other structures are necessary. One of the promising directions of developing high-strength pipe steels is obtaining a crystalline ordered bainitic structure [16–18], instead of the ferritic-pearlitic one. The high strength of this structure in steels with low carbon content is mainly provided by the small size of α-phase crystals and by the significant defect density of the crystalline structure [19,20]. In the process of controlled rolling and other kinds of treatment, the optimal structure with bainitic α-phase can be obtained only if proper cooling conditions are chosen in the temperature range of phase transformation [20–24].

Accelerated cooling makes it possible to improve the strength properties by 40–50 N/mm² for plain steels and by 80–100 N/mm² for alloyed steels containing additives of strong carbide-forming elements. It also makes it possible to eliminate the banded orientation of the structure and to reduce the anisotropy of properties [25–33]. It was found that the properties of steel containing bainite in its structure are determined by the type of bainite itself and depend not only on its quantity, but also on its morphological characteristics [34–39]. However, in spite of a great number of published papers [40–44], it should be noted that reliable approaches to the choice of proper bainitic structure, which can provide both improved strength properties and high ductility and toughness, have not been developed yet. Furthermore, there is no single classification system and commonly accepted interpretation of morphological characteristics of bainitic structures, which are formed during accelerated cooling in low carbon alloyed steels, and their influence on the properties [45–48]. Different terms can be used to identify the same structure, and vice versa, i.e., the same term can be used to identify different structures. Hence, the main objective of this paper is to investigate the influence of the cooling rate on phase transformations, and the structural and morphological characteristics of bainite.

2. Materials and Methods

For the experimental investigation in foundry, rolling, heat treatment, dilatometric, mechanical testing, and metallographic analysis, a pipe steel was chosen with the chemical composition presented in Table 1.

Table 1. Chemical composition of the studied steel (wt.%).

C	Mn	Mo	Cr	Ni	S	P	Other Elements (Al, Cu, V, Nb, Ti)
0.062	1.80	0.120	0.032	0.90	till 0.002	till 0.015	0.53

A number of laboratory experiments were carried out in Thermodeform-MGTU Ltd. (Magnitogorsk, Russia) and at the Nanosteel Research Institute, Nosov Magnitogorsk State Technical University, Magnitogorsk, Russia.

The specimens 10 mm in diameter and 80 mm in length were heated in a vacuum using a Gleeble 3500 complex (Dynamic System Inc., New York, USA), with a heating rate of 1 °C/s, to 1000 °C, with further soaking for 15 min. In order to investigate the breakdown of undercooled austenite, the specimens were cooled with different cooling rates from 0.05 to 150 °C/s. The critical points of steel were defined on the basis of dilatometric tests, which were carried out using the Pocket Jaw module of the complex [49]. This module makes it possible to control the heating rate, time and temperature of heating the specimens, as well as to control the cooling rate. The results of the dilatometric tests were used to draw dilatometric curves illustrating the relationship between the change in the specimen diameter and the temperature, and the bends of the curves were taken as the critical points.

To study the microstructure, the samples were ground polished and etched in 4% nital. To define the qualitative and quantitative characteristics of the structure being formed, the optical microscope Axio Observer (Carl Zeiss Microscopy GmbH, Oberkochen, Germany) and the Thixomet PRO (Thixomet, St. Petersburg, Russia) [50] computer image analysis were used, as well as the scanning electron microscope JSM 6490 LV (JEOL Ltd., Tokyo, Japan). Vickers microhardness was measured at a loading of 1 kg using a Buchler Mikromet hardness measuring instrument (BUEHLER Ltd., Lake Bluff, IL, USA) by indenting a 136 degrees square-based diamond pyramid in accordance with the ASTM E-384.

3. Results

The images of the microstructure of specimens of the investigated steel after cooling with different cooling rates, obtained using an optical microscope, are given in Figure 4.

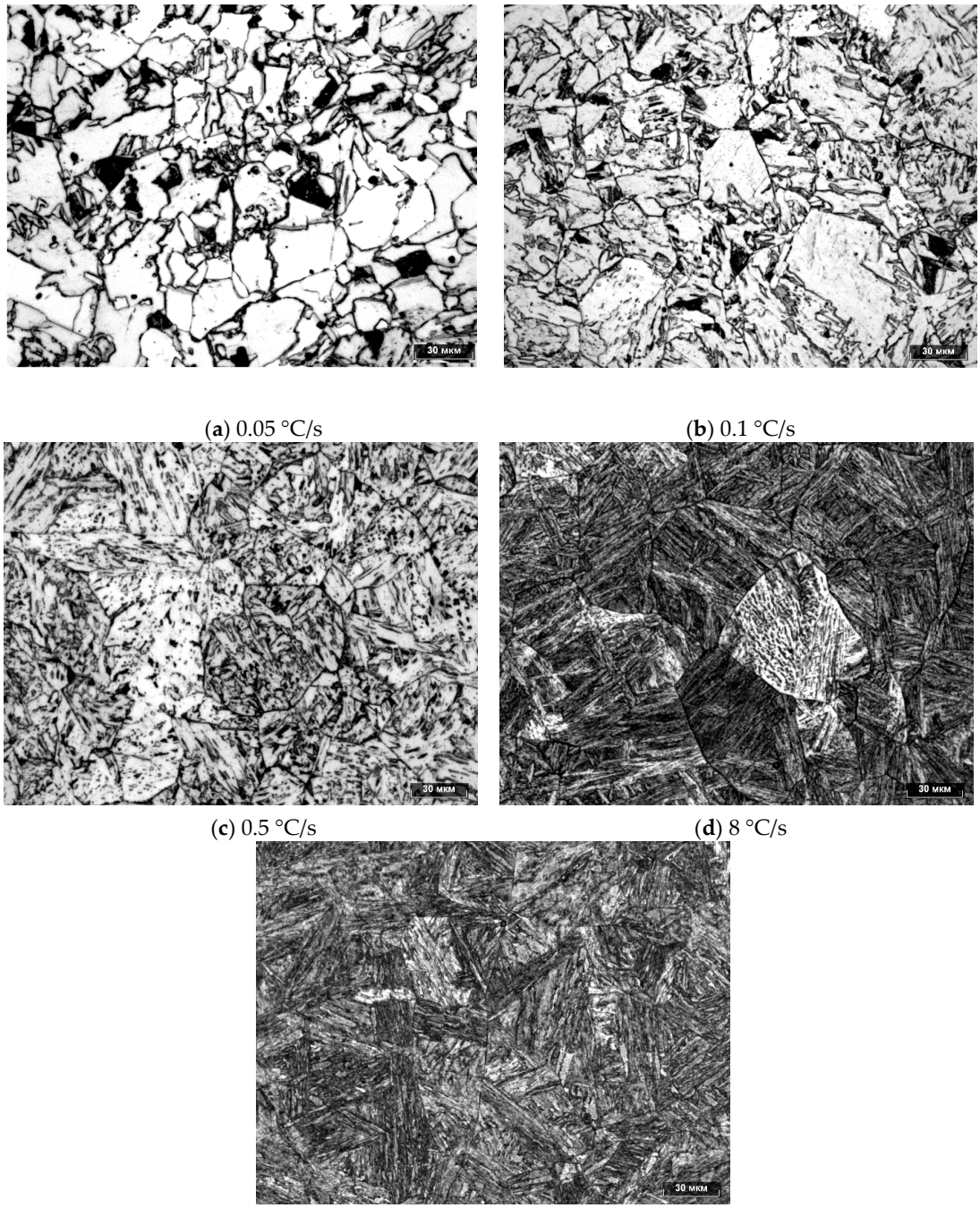

(**a**) 0.05 °C/s (**b**) 0.1 °C/s

(**c**) 0.5 °C/s (**d**) 8 °C/s

(**e**) 75°C/s

Figure 4. Microstructure of the investigated steel after cooling with the following cooling rates: 0.05 °C/s (**a**), 0.1 °C/s (**b**), 0.5 °C/s (**c**), 8 (**d**) and 75 °C/s (**e**).

Analysis of the obtained results shows that at a low cooling rate (from 0.05 to 0.5 °C/s), ferritic-bainitic structure with dark components mostly forms (Figure 4a–c), which as follows from scanning electron microscopy, represents pearlite (P) areas (Figure 5a), areas of martensite-austenite component (MA) and "islands of the second constituent" of the combined type, consisting of pearlitic and MA-components (P + MA) (Figure 5b).

However, the pearlitic areas represent formations without clear alteration of the lamellae of cementite and ferrite. Lamellae of cementite differ in thickness, and they can be bent and divided into separate parts; such pearlite in low carbon steels is referred to as "degenerate" pearlite [16,26,37].

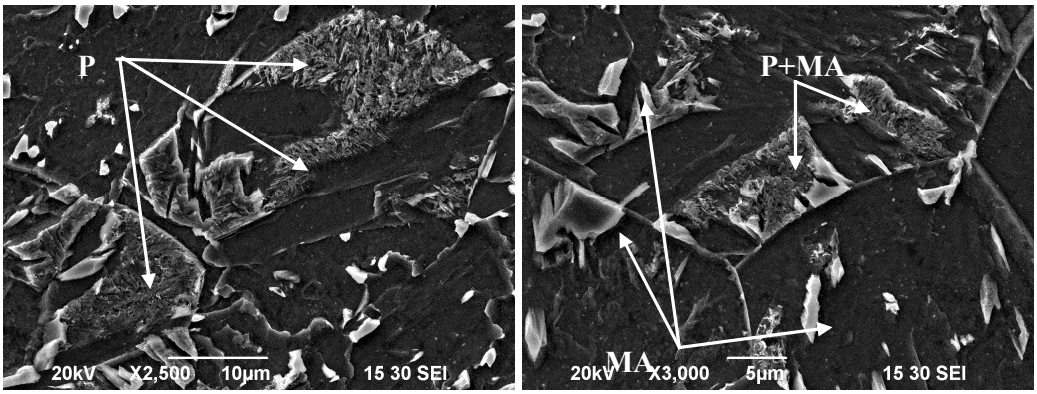

(**a**) (**b**)

Figure 5. Characteristic microstructure of the investigated steel after cooling at rates of 0.05–0.5 °C/s: pearlitic structure (P) (**a**), areas of martensitic–austenitic component (MA) and "islands/areas of the second constituent" of combined type (P + MA) (**b**).

If the cooling rate is higher than 0.5 °C/s, pearlitic transformation was almost completely subdued and, within the investigated range of cooling rates, bainitic structure of various morphology mainly formed (Figure 4c–e).

Scanning electron microscopy was used to define the morphological characteristics of bainite formed at various cooling rates (Figure 6). At low cooling rates from 0.05 to 6 °C/s, bainite forms in the microstructure alongside ferrite. This bainite is usually referred to as granular or globular [37,51,52]. It consists of bainitic α-phase where "islands" of MA-component of 1–5 μm in size are present (Figure 6a). A similar structure of granular (globular) bainite was described by George F. Vander Voort and Bhadeshia H.K. [53,54]. According to some sources, this bainite forms only during continuous cooling [54], while others suggest that it can also form in isothermal conditions [37]. However, granular (globular) bainite always forms in the upper part of the temperature range of the intermediate transformation. In this case, it is probably the temperature range from 700 to 500 °C.

The mechanism of globular bainite formation is not quite clear. It is assumed that during continuous cooling the formed lamellar crystals of bainitic α-phase grow up ("coarsen") and, as a result, they take a shape very similar to the equiaxial one [53,54]. According to other sources, the growth of globular bainite crystals takes place according to the diffusion-controlled step-wise mechanism [37]. While growing, bainite α-phase absorbs the islands with non-transformed austenite with high carbon content. This results in a disordered arrangement of secondary phases (carbides) inside the globular crystals formed during final cooling.

Bainite also occurs in the range of cooling rates from 0.05 to 6 °C/s. Its crystals have an elongated needle-like shape and, in accordance with the classification [37], it is referred to as lower bainite (Figure 6b,c). Crystals of bainitic α-phase up to 1–2 μm wide are commonly parallel (Figure 6b), however, their mutual arrangement can also be quite random (Figure 6c).

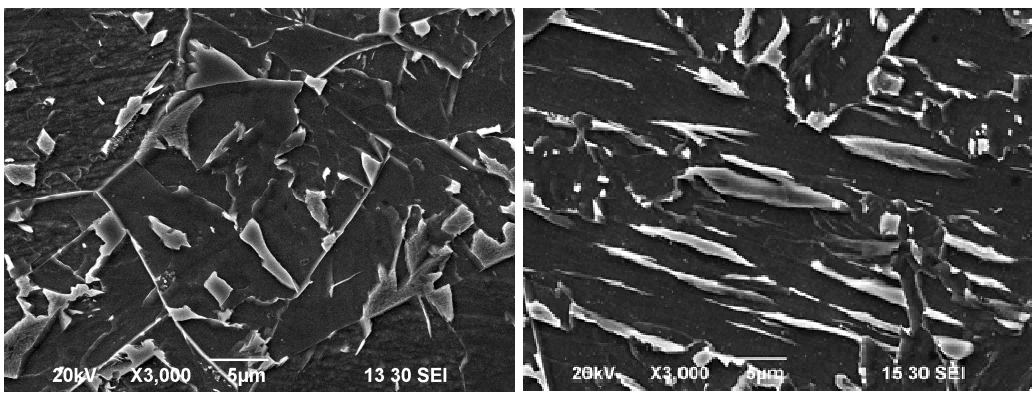

(**a**) 0.1 °C/s (**b**) 0.5 °C/s

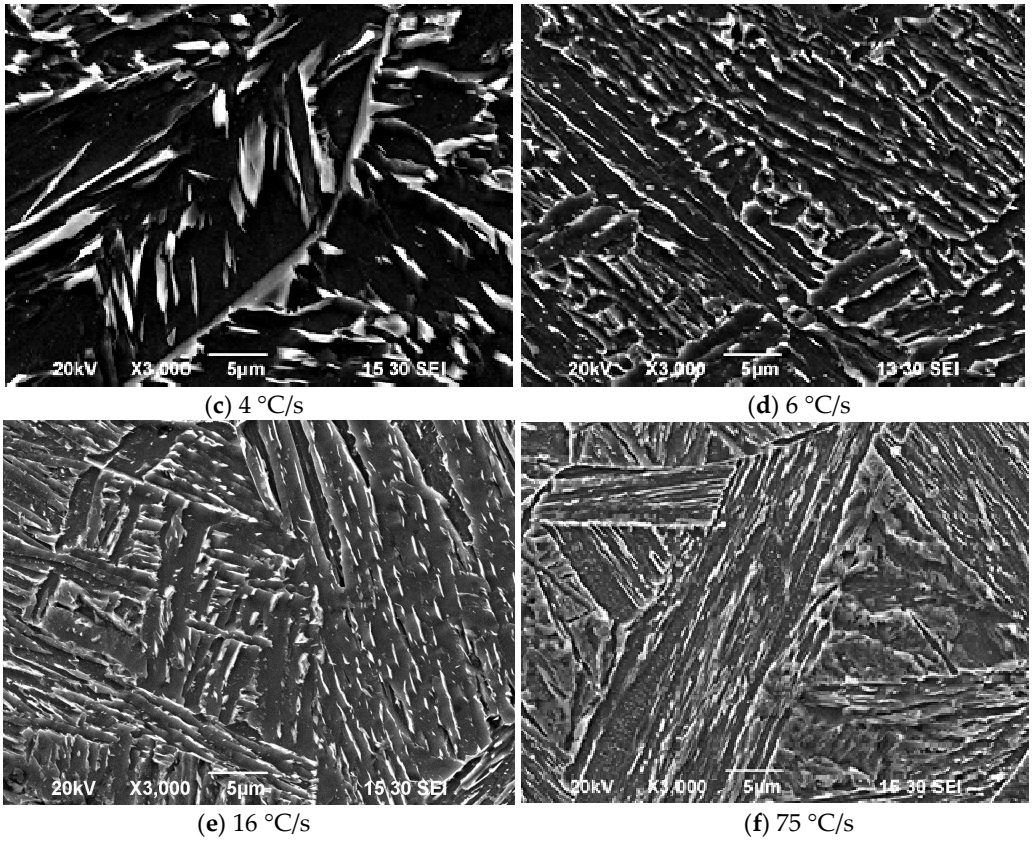

(**c**) 4 °C/s (**d**) 6 °C/s

(**e**) 16 °C/s (**f**) 75 °C/s

Figure 6. Characteristics of bainite in steel after cooling at different cooling rates: 0.1 °C/s (**a**); 0.5 °C/s (**b**); 4 °C/s (**c**); 6 °C/s (**d**); 16 °C/s (**e**); 75 °C/s (**f**).

A similar structure was found by the authors George F. Vander Voort and Bhadeshia H.K., who suggested that granular (globular) and lower bainite form in the same temperature range, however, globular bainite forms at a lower cooling rate than lower bainite [53,54].

At cooling rates of 6–16 °C/s, lath-like bainite forms in the microstructure where the width of laths decreases and they are more evidently arranged in packets (Figure 6d,e). The boundaries of laths are decorated by small particles of "secondary" ones, which are probably carbides and retained austenite.

At cooling rates above 16 °C/s, the type of lath bainite changes, it turns into packet-lath bainite (Figure 6f) [51]. As the cooling rate increases from 50 to 150 °C/s, the average width of laths of bainitic α-phase decreases from 2.22 to 1.34 μm.

Hardness of the specimen cooled at the rate of 0.05 °C/s was 201 HV. This low hardness value can be explained by the presence of ferrite, pearlite and a small amount of bainite. When the cooling rate increases, hardness also increases continuously, which can be explained by the increase in the amount of bainite component.

4. Discussion and Conclusions

Data obtained from dilatometric and structural analyses were used to build the continuous cooling transformation diagram (CCT diagram) of breakdown of undercooled austenite of the investigated steel (Figure 7).

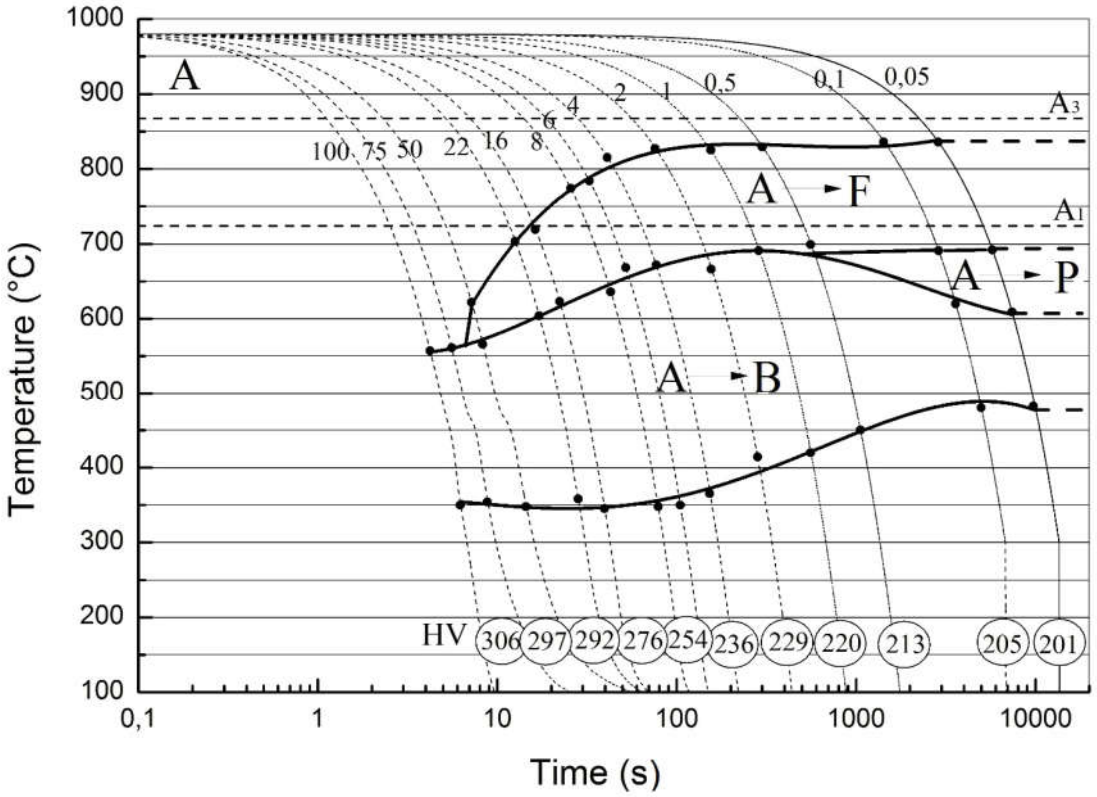

Figure 7. Continuous cooling transformation diagram of breakdown of undercooled austenite of the investigated steel.

At a cooling rate within the range of 1–50 °C/s, the breakdown of the undercooled austenite starts when proeutectoid ferrite forms by a diffusive mechanism at the temperature of 730–720 °C, and the temperature of the start of the formation is clearly detected during dilatometric tests.

When the cooling rate increases, the temperature of the beginning of ferrite formation decreases, and at the cooling rate of 50 °C/s, ferrite formation is subdued completely.

At cooling rates from 0.05 to 0.5 °C/s, pearlite also forms by the diffusion mechanism. Pearlite transformation starts at about 700 °C and stops at about 680 °C. When the cooling rate is above 0.5 °C/s, austenite breakdown and pearlite formation stops completely.

Bainitic transformation developing by the intermediate mechanism takes place within the whole range of the investigated cooling rates from 0.05 to 150 °C/s.

It is well known that bainitic transformation in steel does not proceed to completion. Parts of unchanged austenite remain between the crystals of bainitic α-phase in the process of cooling up to the ambient temperature and can undergo martensite transformation. However, the dilatometric tests carried out within the framework of this research work did not detect any significant increase in the specimen volume, and, consequently, any martensitic transformation point.

The thermal mechanical simulator Gleeble 3500 was used to define the patterns of structural and phase transformations at different cooling rates in steel containing 0.062% C; 1.80% Mn; 0.120% Mo; 0.032% Cr, 0.90% Ni and other elements (Al, Cu, V, Nb, Ti). The research group defined the morphological characteristics of bainite component forming in the range of cooling rates from 0.05 to 100 °C/s. The developed continuous cooling transformation diagram is unique, it has not been found in any reference book, and it can be used to choose the patterns of thermal treatment and thermomechanical processing of the steel of the specified composition.

Author Contributions: P.P. is responsible for general conceptualization; M.G. is responsible for investigation and interpretation of experimental results; M.P. is responsible for formal analysis of experimental results; D.A.

is responsible for conducting experimental research; O.N. is responsible for metallographic observation; D.C. is responsible for experiments on Gleeble 3500; Y.V. is responsible for formal analysis of experimental results.

Funding: The study was financially supported by Ministry of Education and Science of the Russian Federation within the scope of accomplishment of multiple-purpose project on creation of modern high-tech production with the participation of higher education institution (Contract 03.G25.31.0235). The research carried out with the financial support of the grant from the Program Competitiveness Enhancement of Peter the Great St. Petersburg Polytechnic University.

Conflicts of Interest: The authors declare no conflict of interest.

References

1. Gorynin, I.V. Structural materials for Arctic shelf development. *Her. Acad. Sci.* **1999**, *69*, 8–15. (In Russian)
2. Didenko, N.I.; Klochkov, Y.S.; Skripnuk, D.F. Ecological Criteria for Comparing Linear and Circular Economies. *Resources* **2018**, *7*, doi:10.3390/resources7030048.
3. Didenko, N.I.; Skripnuk, D.F.; Kikkas, K.N. The analysis of convergence - divergence in the development of innovative and technological processes in the countries of the Arctic council. In Proceedings of the 2018 International Conference on Information Networking, Chiang Mai, Thailand, 10–12 January 2018; pp. 626–631, doi:10.1109/ICOIN.2018.8343194.
4. Gudkov, A.V.; Dadonov, D.N.; Krotkov, E.A.; Shchepinin, V.E.; Didenko, N.I. Thermal wear of cable lines isolation research owing to current flow of the high harmonics at oil extraction electrical generating systems. In Proceedings of the 2017 6th International Conference on Reliability, Infocom Technologies and Optimization: Trends and Future Directions, ICRITO 2017, Noida, India, 20–22 September 2017; pp. 182–187, doi:10.1109/ICRITO.2017.8342421.
5. Blueprint of Resolution of the Government of the Russian Federation "Strategy for the Development of Arctic Zone of the Russian Federation and Ensuring the National Safety for the Period till 2020 Year" (Ratified by the President of the Russian Federation 18.09.2008 N Пр-1969). Available online: http://legalacts.ru/doc/strategija-razvitija-arkticheskoi-zony-rossiiskoi-federatsii-i/ (accessed on 15 March 2019). (In Russian)
6. Blueprint of Resolution of the Government of the Russian Federation "Basics of the State Policy of the Russian Federation in Arctic Zone for the Period till 2020 Year and Further Perspectives" (Ratified by the President of the Russian Federation 18.09.2008 N Пр-1969). Available online: http://government.ru/info/18359/ (accessed on 15 March 2019). (In Russian)
7. Ruksha, V.V.; Belkin, M.S.; Smirnov, A.A.; Arutunyan, V.G. Structure and dynamics in trucking industry along the North see path: History, the present, and perspectives. *Arct. Ecol. Econ.* **2015**, *4*, 104–110. (In Russian)
8. Nord Stream 2. Programme for the Assessment of the Affect on the Environment. Available online: http://www.greenpeace.org/russia/Global/russia/image/2017/NordStream2-GreenpeaceRussiacomments.pdf (accessed on 15 March 2019) (In Russian)
9. Skripnuk, D.; Ulitin, V.V. Technical and economic substantiation of permafrost thermal stabilization technology under global warming conditions. *Mater. Phys. Mech.* **2016**, *26*, 85–88.
10. Pogodaeva, T.V.; Zhaparova, D.V.; Rudenko, D.Y.; Skripnuk, D.F. Innovations and socio-economic development: Problems of the natural resources intensive use regions. *Mediterr. J. Soc. Sci.* **2015**, *6*, 129–135, doi:10.5901/mjss.2015.v6n1p129.
11. Nikolaev, A.B. Several problems of the Arctic shelf hydrocarbon resources development. *North Mark. Form. Econ. Order* **2016**, *4*, 171–178. (In Russian)
12. King, H.M. Oil and Natural Gas Resources of the Arctic—[Electronic Resort]. Available online: https://geology.com/articles/arcticoil-and-gas/ (accessed on 23 August 2018).
13. Circum-Arctic Resource Appraisal: Estimates of Undiscovered Oil and Gas North of the Arctic Circle [Electronic resort]. Available online: https://pubs.usgs.gov/fs/2008/3049/fs2008–3049.pdf (accessed on 23 August 2018).
14. Forecast for Social and Economic Development of Russia till 2024 Year [Electronic Resort]. Available online: https://acta.tatar/2018/10/07/prognoz-socialno-yekonomicheskogo-ra/ (accessed on 23 August 2018).
15. Afanasyeva, O.V. Analysis of the Investment Programmes of key Enterprises in Thermal and Energetic Complex for Medium-Term Perspective. *Armature Eng.* **2016**, *1*, 36–45. (In Russian)

16. Pumpyanskii, D.A.; Pyshmintsev, I.Y.; Farber, V.M. Strengthening pipe steel. *Steel Transl.* **2005**, *35*, 47–56.
17. Thompson, S.W.; Colvin, D.J.; Krauss, G. Continuous cooling transformations and microstructure in a low-carbon high-strength low-alloy plate steel. *Met. Transl.* **1990**, *21A*, 1493–1507.
18. Bramfitt, B.L.; Speer, J.G. A Perspective on the morphology of bainite. *Met. Transl*. **1990**, *21A*, 817–829.
19. Chukin, M.V.; Poletskov, P.P.; Nikitenko, O.A.; Nabatchikov, D.G. Study of microstructure of rolled heavy plates made of low-alloyed pipe steel with increased strength and cold resistance. *CIS Iron Steel Rev*. **2017**, *13*, 25–31.
20. Efron, L.I.; Il'inskii, V.I.; Golovanov, A.V.; Morozov, Y.D. Production of cold-resistant tube steels by controlled high-temperature rolling. *Steel Transl*. **2003**, *33*, 60–65.
21. DeArdo, A.J. Modern Thermomechanical Processing of Microalloyed Steel: A Physical Metallurgy Perspective. In Proceedings of the International Conference, Microalloying '95, Pittsburgh, PA, USA, 11–14 June 1995; pp. 15–33.
22. Bernshtein, M.L.; Zaimovskiy, V.A.; Kaputkina, L.M. *Thermomechanical Processing of Steel*; Metallurgy: Moscow, Russia, 1983. (In Russian)
23. Efron, L.I. Formation of structures and mechanical properties of constructional steels during thermomechanical treatment in flow of the rolling mill. *Steel Transl*. **1995**, *8*, 57–64.
24. Kodzhaspirov, G.; Rudskoi, A. Thermomechanical processing of steels & alloys as an advanced resource saving technique. In Proceedings of the METAL 2016—25th Anniversary International Conference on Metallurgy and Materials, Hotel Voronez IBrno; Czech Republic, 25–27 May 2016; pp. 248–254.
25. Li, J.-D.; Jiang, Z.-H.; Li, S.-P. Continuous Cooling Transformation Behaviors and Mechanical Properties of High Strength Microalloyed Pipeline Steel. In Proceedings of the International Seminar on Application of High Strength Line Pipe, Xi'an, China, 28–29 June 2010; pp. 126–133.
26. Smirnov, M.A.; Pyshmintsev, I.Y.; Boryakova, A.N. Influence of cooling rate on properties of low-carbon pipe steel. *Bull. South Ural State Univ. Metall*. **2007**, *21*, 15–18. (In Russian)
27. Krauss, G.; Thompson, S.W. Ferritic microstructures in continuosly cooled low- and ultralow carbon steels. *ISIJ Int*. **1995**, *35*, 937–945.
28. Koptseva, N.V.; Chukin, D.M.; Efimova, Yu.Yu.; Nikitenko, O.A.; Ishimov, A.S. Influence of cooling rate on structure forming of rolled wire from 80P steel grade intended for high-tensile reinforcement production. *Ferrous Metals* **2014**, *2*, 23–31. (In Russian)
29. Chukin, M.V.; Poletskov, P.P.; Koptseva, N.V.; Baryshnikov, M.P.; Efimova, Y.Y.; Nikitenko, O.A.; Ishimov, A.S.; Gushchina, M.S.; Bereshnaya G.A. Structural and phase transformations during continuous cooling of high-strength medium carbon complex alloyed low-tempered steels. *Theory Tech. Process Metall. Prod.* **2016**, *1*, 57–62. (In Russian)
30. Chukin, M.V.; Salganik, V.M.; Poletskov, P.P.; Denisov, S.V.; Kuznetsova, A.S.; Berezhnaya, G.A.; Gushchina, M.S. Main types and application fields of strategic high-strength flat products. *Vestn. Nosov Magnitogorsk State Tech. Univ.* **2014**, *4*, 41–44. (In Russian)
31. Rudskoy, A.I.; Kodzhaspirov, G.E.; Kliber, J.; Apostolopoulos, C. Advanced metallic materials and processes. *Mater. Phys. Mech.* **2016**, *25*, 1–8.
32. Kim, Y.M.; Kim, S.K.; Lim, Y.J.; Kim, N.J. Effect of Microstructure on Yield Ratio and Low-Temperature Toughness of Linepipe Steels. *ISIJ Int*. **2002**, *42*, 1571–1577.
33. Gräf, M.; Schröder, J.; Schwinn, V.; Hulka, K. Production of Large Diameter Pipes Grade X70 with High Toughness Using Acicular Ferrite Microstructures. In Proceedings of the International Conference on Application and Evaluation of High Grade Linepipes in Hostile Environments, Yokohama, Japan, 8–9 Novermber 2002, pp. 1–14.
34. Schastlivtsev, V.M.; Koptseva, N.V.; Artemova, T.V. Electron microscopic investigation of martensitic structure in low carbon alloys of iron. *Phys. Met. Phys. Metall.* **1976**, *41*, 1251–1260. (In Russian).
35. Sadovskiy, V.D.; Fokina, E.A.; Schastlivtsev, V.M. *Retained Austenite in Hardened Steel*; Science: Moscow, Russia, 1986. (In Russian)
36. Rodionov, D.P.; Schastlivtsev, V.M.; Stepanova, N.N.; Smirnov, L.V. Shape of martensite crystals in packet (lath) martensite. *Phys. Met. Phys. Metall.* **1986**, *61*, 115–120. (In Russian)
37. Smirnov, M.A.; Pyshmintsev, I.Y.; Boryakova, A.N. Classification of low-carbon pipe steel microstructures. *Metallurgist* **2010**, *54*, 444–454.
38. Efron, L.I.; Il'inskii, V.I.; Morozov, Y.D.; Golovanov, A.V. Tube steel of increased strength and low-temperature stability with predominantly bainite structure. *Steel Transl*. **2003**, *33*, 66–72.

39. Matrosov, Y.I. Development of Principles of Microalloying and Modes of Controlled Rolling of Pearlite-Reduced Steels for Pipes of Gas Transmission Pipelines. Ph.D. Thesis, Bardin Central Research Institute for Ferrous Metallurgy, Moscow, Russia, 1982.
40. Rudskoi, A.I.; Kodzhaspirov, G.; Kliber, J.; Apostolopoulos, C. Thermomechanical processing of steels and alloys physical foundations, resource saving technique and modelling. *Mater. Phys. Mech.* **2018**, *38*, 16–25, doi:10.18720/MPM.3812018_3.
41. Rudskoi, A.I.; Bogatov, A.A.; Nukhov, D.S.; Tolkushkin, A.O. *Mater. Phys. Mech.* **2018**, *38*, 76–81, doi:10.18720/MPM.3812018_11.
42. Rudskoy, A.I.; Bogatov, A.A.; Nukhov, D.S.; Tolkushkin, A.O. New method of severe plastic deformation of metals. *Met. Sci. Heat Treat.* **2018**, *60*, 3–6, doi:10.1007/s11041-018-0231-4.
43. Kodzhaspirov, G.; Rudskoi, A. Simulation of dynamic recrystallization of steels and alloys during rolling and forging through the use of FEM and experimental planning methods. In Proceedings of the METAL 2017—26th International Conference on Metallurgy and Materials, IBrno, Czech Republic, 24–26 May 2017; pp. 320–325.
44. Matveev, M.A.; Kolbasnikov, N.G.; Kononov, A.A. Refinement of the structure of microalloyed steels under plastic deformation near the temperatures of polymorphic transformation. *Met. Sci. Heat Treat.* **2017**, *59*, 197–202, doi:10.1007/s11041-017-0128-7.
45. Davydov, V.V.; Kruzhalov, S.V.; Grebenikova, N.M.; Smirnov, K.Y. Method for determining defects on the inner walls of tubing from the velocity distribution of the flowing fluid. *Meas. Tech.* **2018**, *61*, 365–372, doi:10.1007/s11018-018-1435-0.
46. Bobrynina, E.V.; Larionova, T.V.; Koltsova, T.S.; Ginzburg, S.A.; Michailov, V.G. Effect of alumina addition on weld deposits microstructure at the welding of carbon steel. *Mater. Phys. Mech.* **2018**, *38*, 26–32, doi:10.18720/MPM.3812018_4.
47. Ziniakov, V.Y.; Gorodetskiy, A.E.; Tarasova, I.L. Control of vitality and reliability analysis. *Stud. Syst. Decis. Control* **2016**, *49*, 193–204, doi:10.1007/978-3-319-27547-5_18.
48. Kamyshev, A.V.; Makarov, S.V.; Pasmanik, L.A.; Smirnov, V.A.; Modestov, V.S.; Pivkov, A.V. Generalized coefficients for measuring mechanical stresses in carbon and low-alloyed steels by the acoustoelasticity method. *Russ. J. Nondestruct. Test.* **2017**, *53*, doi:10.1134/S1061830917010090.
49. Borovkov, A.I.; Mamchits, D.V.; Nemov, A.S.; Novokshenov, A.D. Problems of modeling and optimization of variable-hardness panels and structures made of layered composites. *Mech. Solids* **2018**, *53*, 93–100, doi:10.3103/S0025654418010119.
50. Koptseva, N.V.; Chukin, M.V.; Nikitenko, O.A. Use of the Thixomet pro software for quantitative analysis of the ultrafine-grain structure of low-and medium-carbon steels subjected to equal channel angular pressing. *Met. Sci. Heat Treat.* **2012**, *54*, 387–392.
51. Mirzaev, D.A.; Okishev, K.Y.; Schastlivtsev, V.M.; Yakovleva, I.L. The kinetics of formation of bainite and packet martensite. I. Allowance for packet structure. *Fiz. Met. Metalloved.* **2000**, *90*, 55–65.
52. Svishchenko, V.V.; Cheprasov, D.P.; Ivanovskiy, A.A.; Filatov, Yu.A. Phase composition of products of intermediate transformation in 24X2HA steel grade. *Polzunov Bull.* **2005**, *2*, 95–97. (In Russian)
53. Vander Voort, G.F. *Metallography and Microstructures: ASM Handbook*; ASM Int.: Novelty, OH, USA, 2004; p. 9.
54. Bhadeshia, H.K. *Bainite in Steels*, 2nd ed.; Ins. of Materials: London, UK, 2001.